Lee YoungWoo (Orcid ID: 0000-0003-0777-8221)

Article category: Full Paper
Subcategory: Supercapacitor

Engineering geometric electrodes for electric field-enhanced high performance flexible in-plane micro-supercapacitors

Jihong Kim, Sung Min Wi, Jong-Guk Ahn, Sangjun Son, HeeYoung Lim, Yeonsu Park, Hye Ji Eun, Jong Bae Park, Hyunseob Lim, Sangyeon Pak, A-Rang Jang,* Young-Woo Lee,**

J. Kim, S. M. Wi, S. Son, H.Y. Lim, Y. Park, H. J. Eun, Prof. Y.-W. Lee
Department of Energy Engineering, Soonchunhyang University, Asan 31538, Republic of Korea.
E-mail: ywlee@sch.ac.kr

J.-G. Ahn, Prof. H. Lim
Department of Chemistry, Gwangju Institute of Science and Technology, Gwangju 61005, Republic of Korea.

Dr. J. B. Park
Jeonju Centre, Korea Basic Science Institute, Jeonju 54907, Republic of Korea.

Prof. S. Pak
School of Electronic and Electrical Engineering, Hongik University, Seoul 04066, Republic of Korea.
E-mail: spak@hongik.ac.kr

Prof. A-R. Jang
Division of Electrical, Electronic and Control Engineering, Kongju National University, Cheonan 31080, Republic of Korea.
E-mail: arjang@kongju.ac.kr

Keywords: microsupercapcitors, sharp electrodes, electric field enhancement, flexible energy storage device

Abstract

In plane micro-supercapacitors (mSCs) that are miniaturized energy-storage components have attracted significant attention due to their high-power densities for various ubiquitous and sustainable device systems as well as their facile integration on various flexible/wearable platform. To implement the mSCs in various practical applications that can accompany solid state or gel electrolyte and flexible substrates, ions must be readily transported to electrodes for achieving high power densities. Herein, we show large enhancement in electrochemical properties of flexible, in-plane mSC using sharp-edged interdigitated electrode design, which was simply fabricated through direct laser scribing method. The sharp-edged electrodes allowed strong electric field to be induced at the corners of the electrode fingers which led to the greater accumulation of ions near the surface of electrode, significantly enhancing the energy-storage performance of mSCs. The electric field-enhanced in-plane mSC showed the volumetric energy density of 1.52 Wh L^{-1} and the excellent cyclability with capacitive retention of 95.4 % after 20,000 cycles. We further showed various practicability of our sharp-edged design in mSCs by showing circuit applicability, mechanical stability, and air stability. These results present an important pathway for designing electrodes in various energy storage devices.

1. Introduction

The shrinking of the dimensions of electronic devices and the technological trend toward portable, flexible, wearable, sustainable, and Internet-of-things (IoT) devices have spurred to develop miniaturized and multifunctional energy-storage components.[1-8] Micro-supercapacitors (mSC) are highly suitable for such demands because they can be integrated with various devices and flexible/wearable platforms, enable fast charge/discharge operation due to short ion diffusion pathway, and have sufficient power densities for microelectronic applications. Especially, electric double-layer (EDL)-mSCs show fast and reversible charge/discharge processes and long lifetime, suitable for ubiquitous and sustainable device systems. [9-13] In addition, EDL-mSCs can employ same electrode and electrolyte materials employed for supercapacitors and utilize conventionally used microfabrication processes for realization of variety of device and electrode design. In this sense, tremendous efforts have been paid to not only successful utilization of mSC with various applications using materials fabrication routes but also boosting power performances and energy-storage capacities by designing electrode surface area and electrolytes. [14-25]

Common geometries employed for EDL-mSCs are sandwich-type and in-plane interdigitated electrode designs. [25,26] Generally, in-plane interdigitated electrode design allows the EDL-mSCs be thinner, smaller, and more compatible with any substrates, due to simple planar geometry. [26-28] Furthermore, short distance between electrode fingers provides short ion diffusion pathways, and ions can be readily transported to show high power density compared to the sandwiched electrode design. The in-plane interdigitated electrode design is therefore suitable for micropatterned electrodes, facile design of electrode patterns and interspaces, and microscale, high power sources. However, practical applications require solid-state or gel type electrolytes for compact integration with various platforms. In this case, however, ionic conductivity is rather poor, suffering from drawbacks of poor ionic conductivity and low power densities. Therefore, further improvement in the interdigitated

electrodes and electrode pattern design strategies are needed for the prospects of implementation in practical applications and enhance the ion transport and power density of the EDL-mSCs.

In this work, we propose novel mSC electrode design stratedgy by demonstrating electric field-enhanced in-plane mSC using sharp-edged interdigitated electrodes which was simply fabricated using the carbonization of the flexible PI film through direct laser scribing method. To verify the field-enhancement through the electrode design, we employed mSCs with various sharp-edged electrode design having different electrode area and gap distance and compared the electrochemical performance with mSCs having conventionally employed rectangular shape electrodes. The sharp-edged electrode design allowed strong electric field to be induced at the sharp-edged corners, supported through finite-difference time-domain (FDTD) simulation. The strong electric field accumulated at the electrode corners led to a greater accumulation of electrolyte ions near the carbon electrodes and enhancement of energy-storage performance. Further, we observe the circuit applicability of the mSC design through connecting them in series/parallel as well as prove the practical applicability through monitoring the capacitive retention under multiple mechanical bending and long-term cycles tests. This proof-of-concept mSC device represent an important strategy toward designing flexible mSCs and sustainable device systems.

2. Results and discussion

The fabrication of interdigitated carbon-based electrodes is illustrated in **Figure** 1a. carbon-based electrodes were fabricated on polyimide (PI) sheets using a stepwise direct laser scribing method as we previously reported.[20] The direct laser scribing allows the any patterns to be created, which is highly suitable for the design of in-plane mSC electrodes. The pulsed laser immediately carbonizes the PI sheets and form carbon-based electrodes. After the laser carbonization process of cathode and anode electrodes, H_3PO_4/PVA gel electrolyte

composites were drop-coated onto the interdigitated carbon-based electrodes using a micropipette to cover the entire electrode areas. The in-plane mSC with carbon-based electrodes and gel electrolyte was then dried overnight to stabilize the gel electrolyte.

The basic principle of the electrode design and the concept of field-enhanced electrode are captured in Figure 1b. In order to observe the enhancement of mSC performance via electric field, we have designed two interdigitated electrode structures with (1) conventional rectangular pattern and (2) sharp-edged triangular pattern and compared the performance of mSCs so as to clearly verify the effectiveness of strong electric field in the electrode structure. In the sharp-edged triangular pattern, strong electric field is presented at the corner edges of the interdigitated electrodes (Figure 1b left), arising from the accumulation of charges at the sharp edges. The electric field distribution is rather much uniform in rectangle patterned electrodes (Figure 1b right) compared to the sharp-edged triangular pattern. The optical images of the flexible, in-plane mSCs with different electrode design are shown in Figure 1c. Owing to high flexibility of PI sheets and carbon electrodes, the in-plane mSCs can sustain their original device structure even under high mechanical stresses and bending without a noticeable damage as shown in right image of Figure 1c.

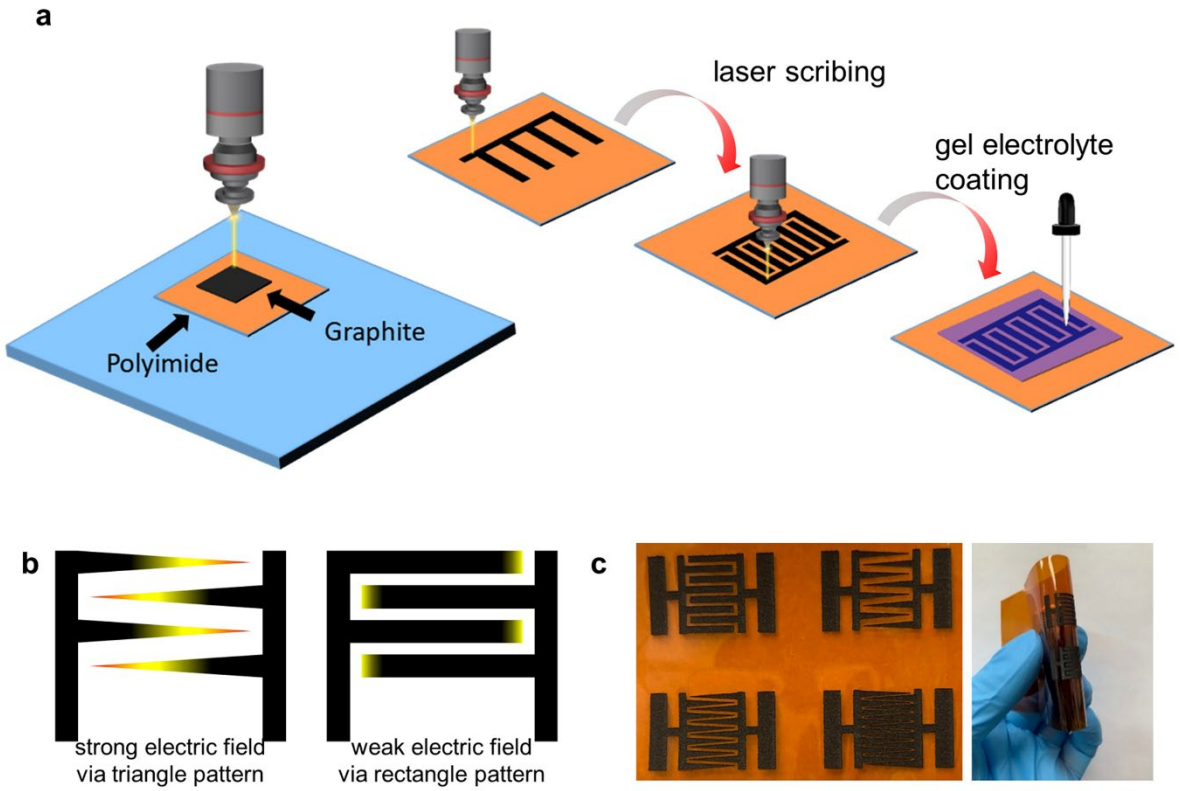

Figure 1. Fabrication of interdigitated carbon-based electrodes. a) Schematic illustration of carbon electrode fabrication on polyimide (PI) sheets using a stepwise direct laser scribing method. The mSCs contain laser-scribed carbon electrodes and H_3PO_4/PVA gel electrolyte composites. b) Schematic illustration of electric field effect in sharp-edged interdigitated electrodes and conventional rectangular interdigitated electrodes. c) The optical image of the fabricated flexible mSCs with different electrode design (mSC-bare, mSC-8, mSC-12, mSC-16).

In order to confirm the effect of sharp-edged electrodes, it is important to fairly compare the electrochemical performance at identical electrode surface area and distance between the electrode fingers. The rectangular interdigitated electrode configuration (mSC-bare, hereafter) has the finger length of 7.5 mm, finger width of 1 mm, gap distance of 0.5 mm, electrode area of 0.83 cm^2, and 8 fingers as shown in **Figure** 2a. Three sharp-edged

interdigitated electrode configuration was designed with (1) 8 identical fingers (mSC-8) and ~2 times longer gap distance and smaller electrode area of 0.53 cm^2 than mSC-bare, (2) 12 fingers (mSC-12) with identical gap distance and smaller electrode area of 0.68 cm^2 than mSC-bare, and (3) 16 fingers (mSC-16) with identical electrode area of mSC-bare (0.83 cm^2). These three sharp-edged interdigitated electrode designs and optical images are shown in Figure 2a and b, respectively. All electrode designs with the carbon electrode showed similar electrical properties as shown in Figure S1.

To evaluate the carbonization of PI film using the direct laser scribing method, the carbon electrodes were characterized using Raman and XPS as shown in Figure 2c,d. Figure 2c shows Raman spectrum of the carbon electrodes with different interdigitated designs. Three strong peaks were shown at 1347 cm^{-1} (D-band), 1587 cm^{-1} (G-band), and 2691 cm^{-1} (2D-band), and two weak peaks were shown at 2458 cm^{-1} (D + D'') and 2938 cm^{-1} (D + D'). [22,23] Typically, the high ratio of intensity of G-band peak and 2D-band peak is a signature of graphite. The intensity ratio I_G/I_{2D} is greater than 1 for all of the interdigitated carbon electrodes. Also, the sharp 2D peak resembles the peak found in typical 2D graphite structure,[32] demonstrating that the PI film was easily converted into graphite composites with layered structures. We also performed X-ray photoelectron spectroscopy (XPS) for the carbon electrodes as shown in Figure 2d. The carbon electrodes exhibited a common graphite characteristic with strong peak shown at 284.02 eV which correspond to C-C peak and is a clear signature of formation of layered graphite structure. Other oxygen-carbon peaks were weakly observed at 289.7 eV (O-C=O) and 285.3 eV (C-O), [33-35] demonstrating the high-quality of the carbon electrodes fabricated using the direct laser scribing method.

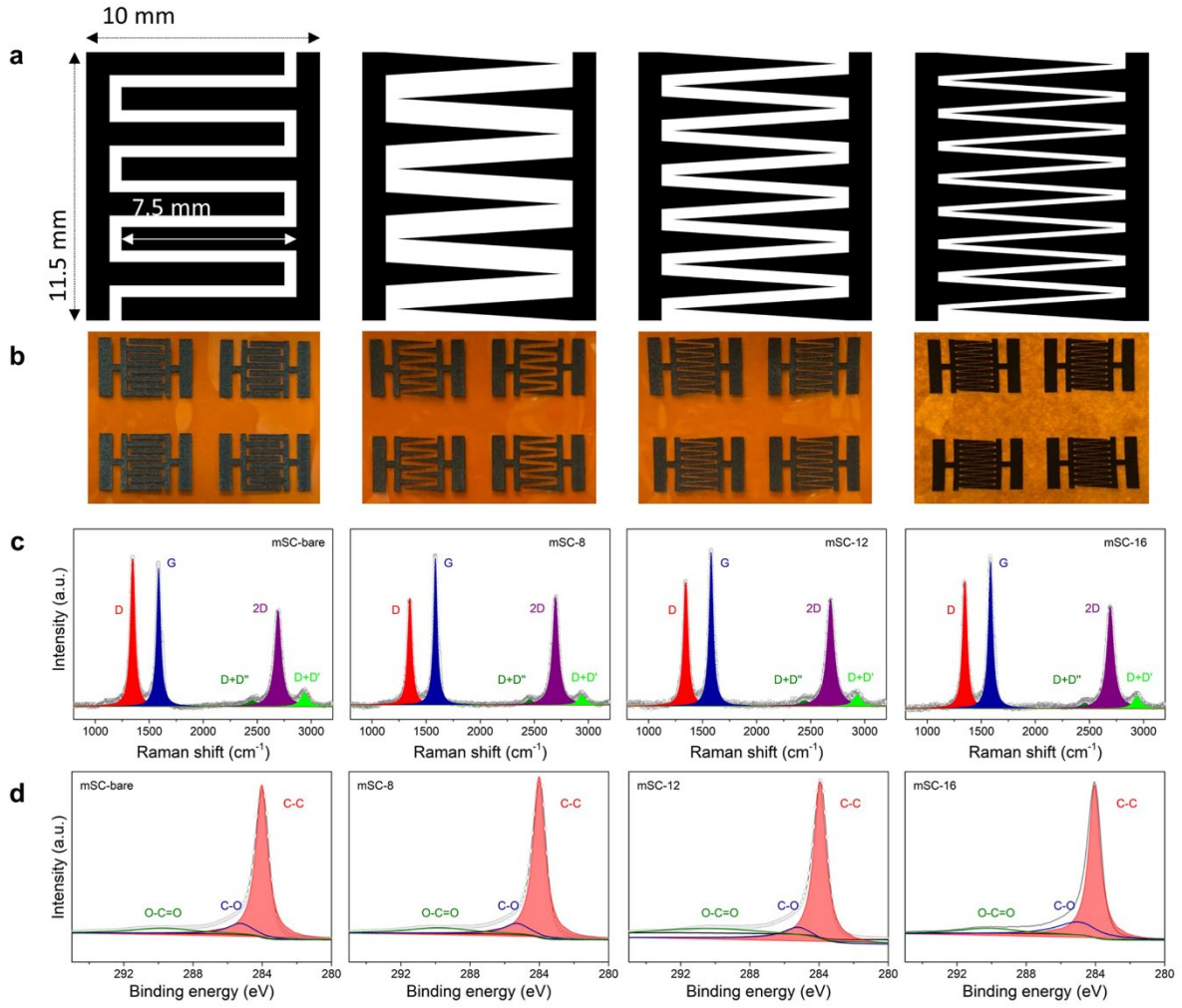

Figure 2. a) Schematic illustration and b) optical images of different interdigitated electrode configuration. mSC-bare has the finger length of 7.5 mm, finger width of 1 mm, gap distance of 0.5 mm, electrode area of 0.83 cm^2, and 8 fingers. mSC-8 has ~2 times longer gap distance and smaller electrode area of 0.53 cm^2 than mSC-bare, mSC-12 has 12 fingers with identical gap distance and smaller electrode area of 0.68 cm^2 than mSC-bare. mSC-16 has 16 fingers with identical electrode area as mSC-bare (0.83 cm^2). c) Raman and d) X-ray photoelectron spectroscopy (XPS) spectrum of carbon electrodes with different interdigitated designs, showing the formation of carbon electrodes using laser-scribed method.

The electric field-enhancement of the mSCs was firstly evaluated by measuring electrochemical properties of the mSCs with conventional rectangular interdigitated

electrodes and sharp-edged interdigitated electrodes. **Figure** 3a-c show the cyclic voltammetry (CV) curves of mSC-8, mSC-12, and mSC-16, respectively, which are plotted together with CV curve of mSC-bare in order to readily compare the energy storage performance. The CV curves were measured at a scan rate of 100 mV s^{-1}. All of the CV curves are nearly rectangular in shape, and there is no obvious oxidation/reduction peaks within a voltage window of 1 V, showing EDL type of CV curves for the carbon electrodes. The area surrounded by CV curves were calculated to be 262.28 μF cm^{-2} for mSC-bare, 233.20 μF cm^{-2} for mSC-8, 408.26 μF cm^{-2} for mSC-12, and 518.03 μF cm^{-2} for mSC-16. It should be noted that even though mSC-8 has longer gap distance and smaller electrode area than mSC-bare, the areal capacitance is similar, and the areal capacitance of mSC-12 is much large than mSC-bare even though the mSC-12 has smaller electrode area and shorter gap distance compared to mSC-bare. These results imply that the electrochemical performance of the mSCs with sharp-electrode design is superior than that of the mSC with conventional rectangular design, and such enhancement can be attributed to the enhancement of electric field from the sharp electrode design.

In order to support electric field-enhancement in the sharp-edged electrode design, the electric field distribution in interdigitated rectangular and sharp-edged electrodes is evaluated using FDTD simulation. The electrode geometries were chosen for similar electrode surface area as mSC-bare, mSC-8, mSC-12, and mSC-16. To clearly compare the magnitude of electric fields, the electric field distribution was depicted with the identical scale bar. From the steady-state analysis of electric field in Figure 3d, it was clearly observed the stronger electric field at the sharp-edged corners due to edge effect. [36] The sharp-edged corner can collect more electric charges in a tiny space with the same applied voltage, leading to a high electric field. Further, an extremely amplified electric field was generated when the gap distance was shorter and the electrode had larger number of electrode fingers.

The stronger electric field in the mSCs with sharp-edged electrodes geometry enhances the energy storage properties through the edge effect. Compared to the rectangular electrodes geometry, sharp-edged electrode geometry has increased electric field intensity or flux, leading to the greater accumulation of electrolyte ions near the carbon electrodes. As the drift of ions under an electric field E can be treated as a classical hydrodynamic reaction (Stokes's law),[37] $\frac{v}{E} = ze/6\pi\eta r_i$, where η is the solvent viscosity, r_i is the ion radius, force on ion is zeE, hydrodynamic resistance is $6\pi\eta r_i\, v$, and v is the ion velocity under electric field E. As the electric field is stronger in mSCs with sharp-edged electrode geometry compared to mSC-bare, the corresponding ion movement is much stronger, and the electrostatic capacitance is enhanced from the greater accumulation of ions near electrodes. Therefore, the edge-effect is crucial in enhancing the performance of the mSCs, especially under gel-type or solid electrolyte where ion conductivity is not high.

The galvanic charge/discharge (GCD) curves of mSC-bare and mSC-16 measured at a current of 1 μA is presented in Figure 3e. GCD of mSC-bare and mSC-16 shows that the charge and discharge time of mSC-16 is much longer than mSC-bare. The calculated area capacitance of mSC-16 (1.306 mF cm^{-2}) was approximately 1.64 times higher than that of mSC-bare (0.798 mF cm^{-2}). In addition, the volumetric capacitance (108.8 F L^{-1}) and energy density (1.52 Wh L^{-1}) of mSC-16 is higher than those of mSC-bare (66.5 F L^{-1} for volumetric capacitance and 0.93 Wh L^{-1} for volumetric energy density) and other reported mSCs (Table S1). The GCD curves of mSC-16 are different current is shown in Figure 3f. Even at the current of 500 μA, the volumetric capacitance of 10.1 F L^{-1} for mSC-16 was achieved. In addition, the energy storage performance of mSC-16 was tested for 10 different samples showing reproducible performance of the mSCs with the sharp electrode geometry.

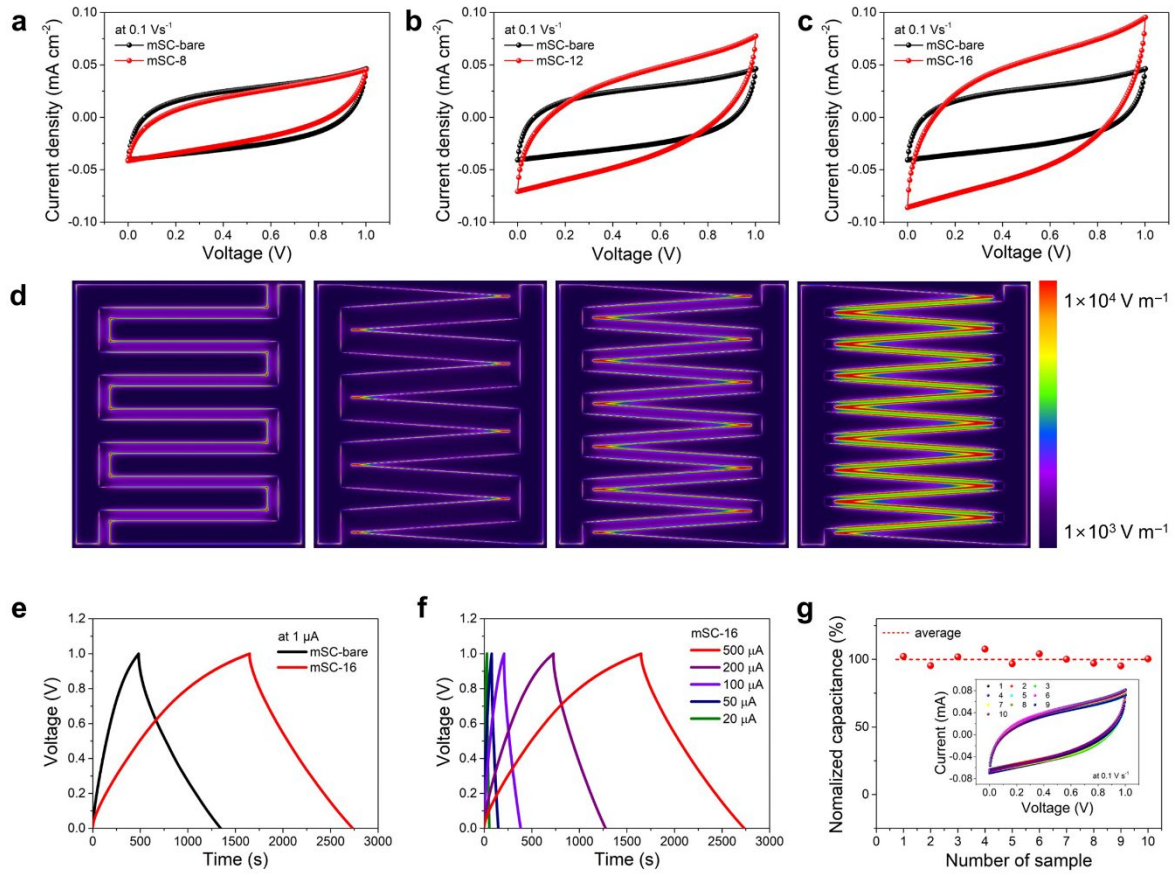

Figure 3. a-c) Cyclic voltammetry (CV) curves of mSC-8, mSC-12, and mSC-16, which are plotted together with CV curve of mSC-bare. Sharp-edged mSCs show higher areal capacitance even though the smaller electrode area or longer gap distance compared to mSC-bare, implying the superiority of the electrode design. d) FDTD simulation showing the distribution of electric field. Electric field becomes stronger as the gap distance and the number of fingers decreases and increases, respectively. e) The galvanic charge/discharge (GCD) curves of mSC-bare and mSC-16 measured at a current of 1 μA. f) The galvanic charge/discharge (GCD) curves of mSC-16 measured under different current. g) Reproducibility of the mSCs with sharp electrode geometry, showing similar capacitance for 10 different samples.

We also evaluated the circuit applicability of the mSCs with sharp-edged electrode geometry by assembling four mSC-16 in series and parallel as shown in **Figure** 4. The operating cell voltage or capacitance is expected to increase proportionally with the series and parallel connection of mSCs. Figure 4a shows the CV curves when multiple mSCs-16 was connected in series. The voltage windows from 1 to 4 mSC cells in series were increased from 1 to 4 V. In addition, when the mSCs were connected in parallel (Figure 4b), the CV currents increased proportionally with increasing the number of cells (from 0.18 mA to 0.70 mA at 1.0 V). The CV results obtained from series and parallel connection of the mSCs with sharp edged geometry demonstrated great possibility of circuit operation for future energy-storing devices.

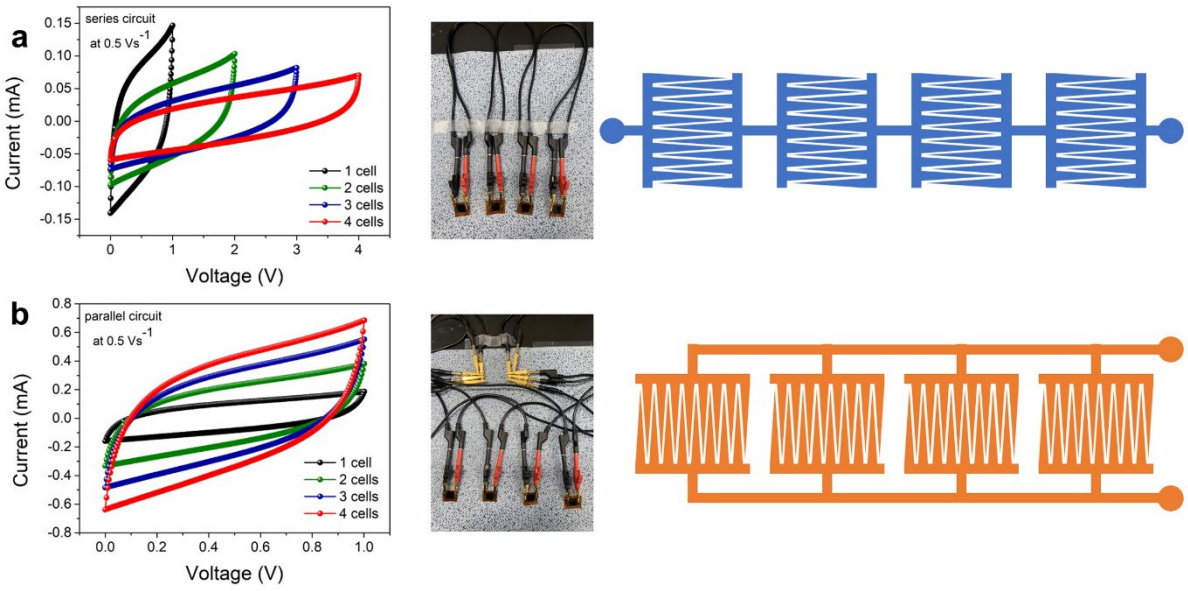

Figure 4. a) Series and b) parallel connection of 4 mSC-16. The operating cell voltage or capacitance increased proportionally with the series and parallel connection of mSCs. The voltage windows increased 1 to 4V when mSCs are connected in series. CV currents increased proportionally from 0.18 mA to 0.70 mA at 1.0 V when the mSCs were connected in parallel.

In addition to circuit applicability of the mSCs, mechanical flexibility and stability of the mSCs with sharp-edged electrode geometry were evaluated under different bending radius and compressive/tensile strain. **Figure** 5a,b show schematic and optical image of applying external strain to the mSCs and the corresponding bending radius from 10 to 5 mm. Figure 5c presents the CV curves measured at a scan rate of 500 mV s^{-1} under different bending radius (5, 6, 7.5, and 10 mm). The CV curves did not show any noticeable degradation in the energy storage performance even though the bending radius reached 5 mm. Furthermore, the CV curves measured at a scan rate of 500 mV s^{-1} did not show any degradation upon the application of tensile and compressive strain with identical bending radius of 5 mm as shown in Figure 5d and 5e. Note that the tensile and compressive strain was applied depending on the position of the mSCs respective to the location of the neutral axis. To further test the mechanical stability of the energy storage performance, the CV curves were measured after multiple bending cycles (tensile strain) up to 1000. Interestingly the stability was reached 97.83% of its original value even up to bending cycles of 1000, showing outstanding mechanical stability of our mSCs with sharp-edged electrode configuration. After the application of diverse external strain, it can be clearly seen that the mSCs can be successfully applied to diverse flexible and wearable applications sowing the high flexibility of carbon and PI substrate.

We further demonstrated air stability and cyclic stability of the mSCs with sharp-edged electrode geometry by monitoring the capacitive retention behavior when the mSCs are measured after multiple weeks and multiple cycles. Figure 5g shows the capacitive stability of the mSCs in air. Due to the structural and material stability of carbon electrodes fabricated using the direct laser scribing method, the capacitive retention was maintained 95.4 % from the original value even after the mSC was measured after 10 weeks. Further, the capacitive stability of the mSCs were measured for multiple cycles up to 20,000, which exhibit a promising capacitive retention of 95.4 % after 20,000 cycles. Moreover, after the capacitive

stability evaluation, it was confirmed that the carbon electrode of mSC maintains high crystallinity of graphite with layered structure, although some surface oxidation was present (Figure S2). These results suggest that the mSCs with carbon electrodes have suitable energy storage performance that can be employed for various sustainable device systems.

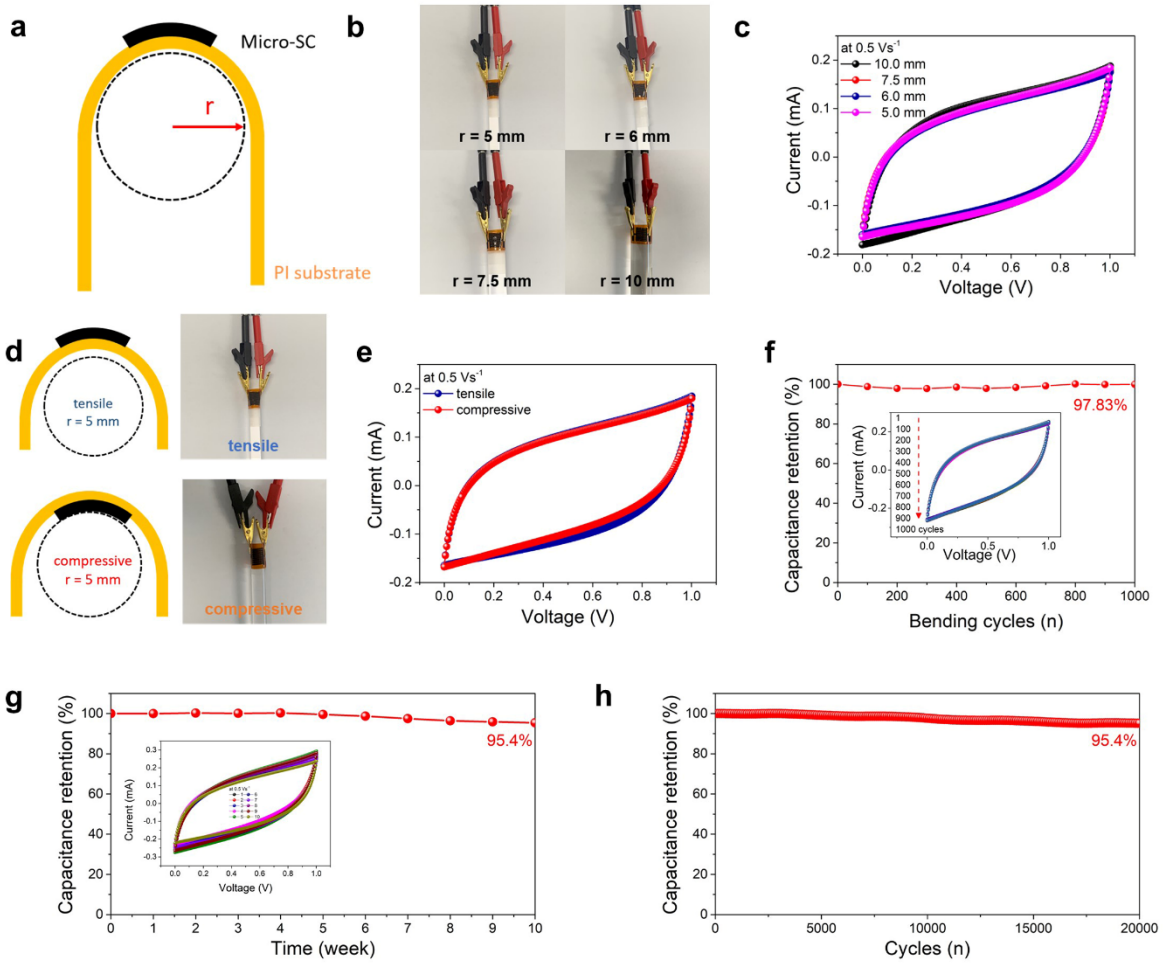

Figure 5. Mechanical and air stability of mSC-16. a) schematic illustration and b) optical image of the mSCs under different bending radius, ranging from 10 to 5 mm. c) CV curves measured under different bending radius (5, 6, 7.5, and 10 mm). The CV curves did not show any noticeable degradation in the energy storage performance even though the bending radius reached 5 mm. d) Application of tensile and compressive strain with identical bending radius of 5 mm e) CV curves measured under tensile and compressive strain. f) Capacitance retention test after multiple bending cycles (tensile strain) up to 1000, reaching 97.83% of its

original value even up to bending cycles of 1000. g) Air stability and h) cyclic stability of the mSCs with sharp-edged electrode geometry by monitoring the capacitive retention behavior when the mSCs are measured after multiple weeks and multiple cycles, showing high stability under both air and multiple cycles.

3. Conclusion

To conclude, we demonstrated the electric field-enhancement of micro-supercapacitors based on carbon electrodes fabricated using laser scribing of PI film. The strong electric field was induced by employing sharp-edged interdigitated electrode instead of conventional rectangular electrode geometry, which was confirmed through FDTD simulation. The electric field-enhanced in-plane mSC showed the volumetric energy density of 1.52 Wh L^{-1} and the outstanding cyclability with capacitive retention of 95.4 % after 20,000 cycles. The effect of sharp-electrode design was demonstrated through enhanced capacitive behaviors achieved through enhanced ion transport to the electrode surface. Furthermore, the feasibility of the sharp electrode applications was demonstrated using series/parallel circuit connection and verifying the high mechanical and air stability of the mSCs. The results demonstrated in this work pave an important pathway toward designing mSCs and sustainable device systems.

Supporting Information

Supporting Information is available from the Wiley Online Library or from the author.

Acknowledgements

This research was supported by a National Research Foundation of Korea grant funded by the Korean government (MSIT) (2020R1A2C1101039) and by Korea Institute of Energy Technology Evaluation and Planning (KETEP) and the Ministry of Trade, Industry, and Energy (MOTIE) of the Republic of Korea (No. 20204030200060). Also, this research was supported by the Soonchunhyang University Research Fund.

† J. Kim and S.M. Wi contributed equally to this work.

Received: (will be filled in by the editorial staff)
Revised: (will be filled in by the editorial staff)
Published online: (will be filled in by the editorial staff)

References

[1] Y. Zhao, H. Liu, Y. Yan, T. Chen, H. Yu, L. O. Ejeta, G. Zhang and H. Duan, *Energy Environ. Mater.* ***2021,*** https://doi.org/10.1002/eem2.12303.

[2] M. Tahir, L. Li, L. He, Z. Xiang, Z. Ma, W. A. Haider, X. Liao and Y. Song, *Energy & Environmental Materials. 2022,* https://doi.org/10.1002/eem2.12546.

[3] T. Kim, S. Pak, J. Lim, J. S. Hwang, K. -H. Park, B. -S. Kim, S. Cha, *ACS Appl. Mater. Interfaces* **2022,** *14,* 13499-13506.

[4] X. Wang, X. Lu, B. Liu, D. Chen, Y. Tong, G. Shen, *Adv. Mater.* **2014,** *26,* 4763.

[5] J. Lim, T. Kim, J. Byeon, K. -H. Park, J. Hong, S. Pak, S. Cha, *J. Mater. Chem. A* **2022,** *10,* 23274-23281.

[6] C. Yang, R. Gao, H. Yang, *EnergyChem*, **2021**, *3.5*, 100062.

[7] D. Li, S. Yang, X. Chen, W. Y. Lai, W. Huang, *Adv. Functional Mater*, **2021**, *31(50)*, 2107484.

[8] X. Liu, D. Li, X. Chen, W.-Y. Lai, W. Huang, *ACS applied materials & interfaces*, **2018**, *10(38)*, 32536-32542.

[9] P. Xie, W. Yuan, X. Liu, Y. Peng, Y. Yin, Y. Li, Z. Wu, *Energy Storage Mater.* **2021,** *36*, 56.

[10]Z.-S. Wu, X. Feng, H.-M. Cheng, *Natl. Sci. Rev.* **2014**, *1*, 277.

[11]Y. Shao, M. F. El-Kady, L. J. Wang, Q. Zhang, Y. Li, H. Wang, M. F. Mousavi, R. B. Kaner, *Chem. Soc. Rev.* **2015**, *44*, 3639.

[12]V. Vandeginste, *Appl. Sci.* **2022**, *12*, 862.

[13] L. Liu, D. Ye, Y. Yu, L. Liu, Y. Wu, *Carbon* **2017**, *111*, 121.

[14] H. U. Lee, S. W. Kim, *J. Mater. Chem.-A* **2017**, *5*, 13581.

[15] Y. Park, H. Choi, D.-G. Lee, M.-C. Kim, N. A. T. Tran, Y. Cho, Y.-W. Lee, J. I. Sohn, *ACS Sustain. Chem. Eng.* **2020**, *8*, 2409.

[16] C. Shen, X. Wang, S. Li, W. Zhang, F. Kang, *J. Power Sources* **2013**, *234*, 302.

[17] T. Purkait, G. Singh, N. Kamboj, M. Das, R. S. Dey, *J. Mater. Chem.-A* **2018**, *6*, 22858.

[18] S. H. Lee, J. Lee, J. Jung, A. R. Cho, J. R. Jeong, C. Dang Van, J. Nah, M. H. Lee, *ACS Appl. Mater. Interfaces* **2021**, *13*, 18821.

[19] S. Zhu, M. Göbel, P. Formanek, F. Simon, M. Sommer, S. Choudhury, *J. Mater. Chem.-A* **2021**, *9*, 14052.

[20] S. M. Wi, J. Kim, S. Lee, Y.-R. Choi, S. H. Kim, J. B. Park, Y. Cho, W. Ahn, A.-R. Jang, J. Hong, *Nanomaterials* **2021**, *11*, 3027.

[21] Y. Bai, C. Liu, T. Chen, W. Li, S. Zheng, Y. Pi, Y. Luo, H. Pang, *Angewandte Chemie*, **2021**, *133(48)*, 25522-25526.

[22] S. Zheng, Y. Sun, H. Xue, P. Braunstein, W. Huang, H. Pang, *National science review*, **2022**, *9(7)*, nwab197.

[23] S. Zheng, Q. Li, H. Xue, H. Pang, Q. Xu, *National science review*, **2020**, *7(2)*, 305-314.

[24] D. Li, X. Liu, X. Chen, W. Y. Lai, W. Huang, *Advanced Materials Technologies*, **2019**, *4(8)*, 1900196.

[25] D. Li, W. Y. Lai, F. Feng, W. Huang, *Advanced Materials Interfaces*, **2021**, *8(13)*, 2100548.

[26] P. Li, T. Shang, X. Dong, H. Li, Y. Tao, Q. H. Yang, *Small* **2021**, *17*, 2007548.

[27] B. Yao, J. Zhang, T. Kou, Y. Song, T. Liu, Y. Li, *Adv. Sci.* **2017**, *4*, 1700107.

[28] P. Zhang, F. Wang, S. Yang, G. Wang, M. Yu, X. Feng, *Energy Storage Mater.* **2020**, *28*, 160.

[29] N. Liu, Y. Gao, *Small* **2017**, *13*, 1701989.

[30] S. Roscher, R. Hoffmann, O. Ambacher, *Anal. methods* **2019**, *11*, 1224.

[31] L. Chong, H. Guo, Y. Zhang, Y. Hu, Y. Zhang, *Nanomaterials* **2019**, *9*, 372.

[32] G. Greczynski, L. Hultman, *Prog. Mater. Sci.* **2020**, *107*, 100591.

[33] J. Lin, Z. Peng, Y. Liu, F. Ruiz-Zepeda, R. Ye, E. L. G. Samuel, M. J. Yacaman, B. I. Yakobson, J. M. Tour, *Nature Commun.* **2014,** *5,* 5714.

[34] M.-C. Kim, Y.-W. Lee, S.-J. Kim, B.-M. Hwang, H.-C. Park, E.-T. Hwang, G. Cao, K.-W. Park, *Electrochim. Acta* **2014**, *147*, 241.

[35] A. Dolgov, D. Lopaev, C. J. Lee, E. Zoethout, V. Medvedev, O. Yakushev, F. Bijkerk, *Appl. Surf. Sci.* **2015**, *353*, 708.

[36] J. Meixner, *IEEE Trans. Antennas Propag.* **1972**, *20*, 442.

[37] B. Pal, S. Yang, S. Ramesh, V. Thangadurai, R. Jose, *Nanoscale Adv*. **2019**, *1*, 3807.